Sustainable Food Technology

ROYAL SOCIETY OF CHEMISTRY

PAPER

View Article Online
View Journal | View Issue

Cite this: *Sustainable Food Technol.*, 2026, **4**, 3311

Valorisation of starch-rich pea byproduct into cold-extruded rice analogues: effects of processing temperature on physicochemical, functional, cooking, and *in vitro* digestibility properties

Smriti Chaturvedi,*[a] Prudhvi Pasumarthi,*[a] Mathad P. F.[b] and Annamalai Manickavasagan*[a]

The starch-rich fraction (SRF) from pea protein fractionation is a major underutilized byproduct, and its valorisation is critical for sustainable pulse processing. This study aimed to upcycle SRF into rice analogues using cold extrusion at 25 and 50 °C. Uniformly kneaded SRF (35% added water) was extruded through a rice-shaped die, cut, and dried. The developed analogues were analyzed for nutritional, physicochemical, structural, thermal, cooking, and *in vitro* digestibility properties. Conventional rice was used as the control. The rice analogues exhibited acceptable physical properties and superior nutritional quality with significantly higher protein content (9.4–11%) than the control (3%). Both extrusion conditions produced analogues with reduced crystallinity (25–27%), lower gelatinization temperatures, and shorter cooking times (2–13 min), although they exhibited slightly higher solid loss during cooking (3.3–3.7%). The extruded products also contained a higher amount of resistant starch (11–15%), resulting in a lower expected glycemic index (76–79) compared to the control (85). Among the treatments, extrusion at 50 °C produced the most pronounced effects. Therefore, RAs developed from SRF provide a potential solution for starch-rich byproduct utilization, yielding rice with enhanced nutritional quality, shorter cooking time, and acceptable cooking stability. Processing at moderate temperatures (25 °C) preserves nutritional quality and results in a lower eGI, whereas higher extrusion temperatures (50 °C) enhance convenience through rapid gelatinization and reduced cooking time but compromise nutritional quality and cooking stability.

Received 16th November 2025
Accepted 9th March 2026

DOI: 10.1039/d5fb00902b

rsc.li/susfoodtech

Sustainability spotlight

This work addresses a key sustainability challenge in pulse processing by transforming the underutilized starch-rich fraction (SRF) from pea protein fractionation into value-added rice analogues. Upcycling SRF minimizes industrial waste, improves resource efficiency, and supports a circular bioeconomy. The rice analogues produced in this study showed improved nutritional quality with higher protein and resistant starch, resulting in a lower glycemic index compared to conventional rice, contributing to the social pillar of sustainability. Converting a low-value byproduct into a nutrient-dense staple also strengthens the economic and environmental pillars by adding value to processing streams and reducing waste. This study benefits pulse processors, food manufacturers, and consumers seeking affordable, sustainable, and health-promoting food options.

1 Introduction

The growing global population has increased the demand for sustainable protein sources. As concerns over the environmental impact of animal proteins rise, there has been a major shift toward plant-based alternatives.[1] Among these, legumes are highly valued for their rich protein content. Pulses, a subgroup of legumes, represent the second most preferred industrial source of plant-derived proteins after soybean.[2] Canada is a global leader in pulse production, with peas accounting for 2609 thousand tonnes in 2023–2024 and projected to reach 3200 thousand tonnes by 2025–2026.[3] Pea is widely researched and industrially utilized due to its low allergenicity and relatively complete essential amino acid profile.[4,5] Commercial pea protein is predominantly produced through dry fractionation methods such as air classification or triboelectric separation, with dry fractionation being the most established at an industrial scale.[6] Regardless of the method used, these processes generate a starch-rich byproduct containing 60–75% starch and up to 15% protein.[7] This fraction remains underutilized despite its nutritional potential, underscoring the need for innovative valorisation strategies.

[a]*College of Engineering, University of Guelph, Ontario, Canada. E-mail: schatu01@uoguelph.ca; pasumarv@uoguelph.ca; mannamal@uoguelph.ca*
[b]*Department of Processing and Food Engineering, College of Agricultural Engineering, UAS Raichur, Karnataka, India*

Rice analogues are designed to mimic the physical and functional properties of conventional rice, but from non-paddy carbohydrates.[8] In recent years, interest in rice analogues has grown, driven by the nutritional limitations of conventional rice (*Oryza sativa* L.), which is typically characterized by a high glycemic index and low levels of protein and dietary fiber. To overcome these limitations, a wide range of carbohydrate sources such as corn,[9] sweet potato,[10] cassava,[11] sago,[12] sorghum,[13] kidney bean,[14] mung bean,[15] soybean,[16] pea,[17] and kodo millet[18] flours have been investigated for analogue rice production. The starch-rich pea fraction, a byproduct of protein fractionation, represents a promising raw material for analogue rice due to its relatively high protein content and slowly digestible starch, which arises from the characteristically high amylose levels in pulses (30–56%).[19]

Processing methods, in addition to ingredient composition, play a crucial role in determining the quality attributes of rice analogues. Among the available methods, granulation and extrusion are the most widely used, with extrusion generally producing rice analogues of superior textural and functional quality compared to granulation.[8,20] Extrusion can be further classified into cold and hot processes. Cold extrusion involves pressing the dough through a rice analogue die, whereas hot extrusion applies elevated barrel temperatures (>70 °C) and pressures, facilitating partial cooking during processing.[21] These two approaches yield products with distinct physical and functional properties. Cold extrusion (<70 °C), in particular, offers a simple processing method that minimizes potential thermal damage to nutrients and avoids undesirable functional alterations. Although several studies have investigated rice analogues produced using either extrusion method with various ingredients, to our knowledge, no study has directly examined the effects of cold extrusion at different processing temperatures on rice analogue properties. The novelty of this work lies in evaluating the suitability of the starch-rich pea byproduct from protein fractionation, an underutilized ingredient with the potential to generate additional revenue for pulse processors while contributing to the circular bioeconomy. Further, the properties of rice analogues influenced by extrusion type were also compared with conventional rice (control) to assess their utilization potential from the consumer's perspective.

2 Experimental

2.1 Raw materials

Air fractionated yellow pea starch-rich flour (SRF) was obtained from P&H Milling Group, Guelph, Ontario, Canada. This raw pea starch-rich fraction contained 12% moisture, 2.5% ash, 12% protein, and 65% starch on a dry basis (db). The control white rice grains (*Swarna Cv.*) were procured from a local Indian supermarket. All the chemicals used in this study were of analytical grade and were purchased from Thermo Fisher Scientific (New Hampshire, USA) and Sigma-Aldrich (Missouri, United States).

2.2 Rice analogue preparation

Rice analogues were developed by extrusion processing using a single screw tabletop extruder (*La Monferrina*, Dolly mini, Italy). The processing conditions for extrusion trials were determined based on preliminary trials, which produced rice analogues with desirable texture and shape. The extruder had a single heating zone, a 3 : 1 barrel length-to-diameter ratio, a 227 mm long screw with a 33.5 mm diameter, and was powered by a 2.25 kW electric motor. The extruder die was fabricated to match the typical dimensions of a whole rice grain, with a die hole length of 6.0 mm and width of 2.0 mm at the centre. The dimensions were kept slightly larger than those of a rice kernel to account for shrinkage during drying.[22] To produce rice analogues, SRF was mixed with 35% water (weight of water relative to SRF weight), followed by uniform kneading at 500 rpm for 20 min.[1] The feed rate and screw speed for extrusion were set at 1.5 kg h^{-1} and 55 rpm, respectively.[1] The barrel zone temperature near the shaping die was set at 25 °C and 50 °C for extrusion. These temperatures were selected because extrusion below 25 °C did not produce a product with desirable characteristics, whereas temperatures above 50 °C could lead to adverse thermal effects. A cutting blade, moving at a speed of 90 rpm, was attached to the outlet of the die to produce the rice analogues with desirable dimensions. The extrudates were then collected and equilibrated to room temperature before tray drying at 40 °C to a moisture content of 10–11% (overnight drying). The dried extrudates were packed in air-tight pouches and stored in a desiccator at room temperature for further analysis.

Three samples were considered in this study, including cold-extruded rice analogues at 25 °C (RA 25) and 50 °C (RA 50) and conventional rice (control), to evaluate the effect of extrusion temperature on the quality attributes of SRF-based rice analogues.

2.3 Physico-chemical properties of extrudates

2.3.1 Length–breadth (*L*/*B*) ratio. The dimensions (length and breadth in mm) of thirty individual grains were noted using a vernier calliper, and the value of *L*/*B* was determined as the ratio of length and breadth. An average of *L*/*B* for the 30 kernels was considered.[22]

2.3.2 Bulk density (BD). A known weight (100 g) of the uncooked sample was transferred to a measuring cylinder. The volume occupied was noted, and the bulk density was calculated by dividing the weight (g) by the occupied volume (mL).[23]

2.3.3 True density (TD). The TD of the samples was evaluated using the toluene displacement method. 5 g of the uncooked rice samples was added to 10 mL toluene in a measuring cylinder. True density was determined by the ratio of the weight of the sample to the volume of toluene displaced.[24]

2.3.4 Porosity. Porosity was determined based on true and bulk densities as per eqn (1):[23]

$$\text{Porosity}(\%) = \frac{\text{TD} - \text{BD}}{\text{TD}} \times 100 \quad (1)$$

2.3.5 Color. The color of rice analogue grains was measured in terms of L^* (light/dark), a^* (red/green), and b^* (yellow/blue) values using a colorimeter (Model: CM-5, M/s. Konica Minolta, Japan) after calibrating the instrument with

standard white and black tiles. The change in color (ΔE) was estimated using eqn (2)

$$\Delta E = \sqrt{(L - L^*)^2 + (a - a^*)^2 + (b - b^*)^2} \quad (2)$$

where L, a, and b represent the color values of the reference.

2.3.6 Proximate analysis. Moisture content was measured gravimetrically using the hot air oven method, which involved drying the sample at 105 °C till a constant weight was reached.[25] Ash content was measured using a muffle furnace at 600 °C.[25] The protein content was analyzed using a LECO system (FP828 P, Leco, Michigan, United States) using the Dumas method.[26] The system was initially calibrated using an EDTA standard before analyzing the extruded rice analogues. A nitrogen-to-protein-conversion factor of 6.25 was used to estimate the protein content (%). The total fat content was estimated by the Soxhlet method using hexane as the solvent.[25] The total carbohydrate content was determined using eqn (3):[11]

$$\text{Total carbohydrate (\%, db)} = 100 - (\text{ash} + \text{protein} + \text{fat}) \quad (3)$$

2.4 Functional properties of the extrudates

2.4.1 Water absorption and solubility index. The water absorption index (WAI) and the water solubility index (WSI) were calculated according to the protocol mentioned by Tabas *etal.* (2023).[27] In brief, rice samples (2 g) were ground using a mortar and pestle until the material was sufficiently fine to pass through a 106 μm sieve (ASTM No. 140). The resultant ground material was dispersed in 20 mL of distilled water at ambient temperature and stirred for 20 min, followed by centrifugation at 860 g for 20 min. The weight of the sediment was noted, and the supernatant was dried at 105 °C for 24 h. The WSI and WAI were calculated using the following equations:

$$\text{WAI}\left(\frac{\text{g}}{\text{g}}\right) = \frac{\text{weight of sediment(g)}}{\text{weight of flour sample(g)}} \quad (4)$$

$$\text{WSI}(\%) = \frac{\text{weight of dried supernatant(g)}}{\text{weight of flour sample(g)}} \times 100 \quad (5)$$

2.4.2 Crystallinity. An X-ray diffractometer (Panalytical Empyrean, Malvern, UK) was used to examine the crystallinity of extruded rice analogue flour. The diffractogram was generated over a diffraction angle (2θ) range from 5° to 40° at a step speed of 2.68° min^{-1}.[23] The peaks of crystalline and amorphous regions in the X-ray spectra were identified using OriginPro 2025 software. The crystallinity (%) was determined using eqn (6):

$$\text{Relative crystallinity}(\%) = \frac{\text{area under crystalline peak}}{\text{area under crystalline peak} + \text{area under amorphous peak}} \times 100 \quad (6)$$

2.4.3 Fourier transform infrared spectrophotometry. An Attenuated Total Reflectance-Fourier transform infrared spectrophotometer (ATR-FTIR) (Spectrum 4000 series, PerkinElmer, Massachusetts, US) was used to study the short-range molecular structure of extruded rice analogue samples. The spectral scans were performed in a wavenumber range of 4000 to 400 cm^{-1} with 4 cm^{-1} resolution. The obtained spectra were analyzed using OriginPro 2025 software.

2.4.4 Thermal characteristics. A differential scanning calorimeter (DSC 4000, PerkinElmer, Massachusetts, US) was used to examine the gelatinization properties of the developed rice analogues. An empty aluminium pan was used as the reference. In brief, 2–10 mg of rice analogue flour was mixed with water (1 : 0.65) and equilibrated overnight to adjust the moisture content to 85%. The equilibrated samples were sealed in aluminium pans and subjected to heating in a temperature range of 10–200 °C at a heating rate of 10 °C min^{-1}. The onset (T_o), peak (T_p), and conclusion temperatures (T_c) were determined using Pyris software (PerkinElmer).[27]

2.5 Cooking characteristics

The extruded rice analogue samples were cooked in boiling water (~100 °C) using the traditional open-pan method until the desired state was achieved, defined by the absence of an opaque core when pressed. The cooked samples were then gently surface-blotted with dry tissue paper prior to evaluating the following properties.

2.5.1 Cooking time (CT). The cooking time (min) was determined by compressing cooked grains between two glass slides. It was defined as the time required for the complete disappearance of the opaque core, indicating complete gelatinization.[27]

2.5.2 Elongation ratio. The length of the cooked kernels ($n = 30$) was measured using a vernier calliper and the elongation ratio was measured using eqn (7):[18]

$$\text{Elongation ratio} = \frac{\text{average length of cooked rice kernels}}{\text{average length of uncooked rice kernels}} \quad (7)$$

2.5.3 Water absorption capacity. The water absorption capacity (WAC) is the ability of the grain to retain water after hydration. It was evaluated using the protocol by Tabas *et al.* (2023). The cooked samples were cooled to room temperature, and the weight gain was recorded to measure the water absorption capacity using eqn (8):

$$\text{WAC}(\%) = \frac{\text{weight of cooked rice kernels} - \text{weight of uncooked rice kernels}}{\text{weight of uncooked rice kernels}} \times 100 \quad (8)$$

2.5.4 Solid loss (%). Solid loss or cooking loss was evaluated using eqn (9):[18]

$$\text{Solid loss}(\%) = \frac{\text{dry weight of cooking water(g)}}{\text{weight of uncooked sample(g)}} \times 100 \quad (9)$$

2.5.5 Texture. The textural properties (hardness, adhesiveness, cohesiveness, springiness, chewiness, gumminess, and resilience) of the cooked rice samples were evaluated using a texture analyzer (Texture Technologies Corp., Model: TAXT-PlusC, New York, NY) attached with a 50 kg load cell. A standard two-cycle compression program, with the pretest, test, and post-test speeds set at 1 mm s^{-1}, was used. A 49 mm cylindrical probe was used, and ten rice kernels were compressed for a single run using 70% compression force.

2.5.6 Morphology. The morphology of the cooked and uncooked rice analogues was studied at the surface and transverse section *via* a scanning electron microscope (FEG 250 SEM, FEI Quanta, Oregon, US). For the transverse section, the samples were dissected cautiously using a sharp blade and placed over the carbon tape. The cooked grains were sectioned and dried overnight (~12 h) in a tray dryer (Omcan Instruments, Ontario, Canada) at 30 °C before analysis. The samples were then subjected to gold–palladium sputter coating. The scanning electron microscopy (SEM) images for each sample were captured at an acceleration voltage of 15–20 kV and magnification levels of 100×, 500×, and 2000×.

2.5.7 *In vitro* starch digestibility and expected glycemic index (eGI). The rapidly digestible starch (RDS), slowly digestible starch (SDS), total digestible starch (TDS) and resistant starch (RS) of cooked rice analogues were evaluated using a digestible and resistant starch kit (K-DSTRS) from Megazyme (Wicklow, Ireland) and the protocol suggested in ref. 28. The process involved hydrolysis with pancreatic α-amylase and amyloglucosidase for 0, 10, 20, 30, 60, 90, 120, 180, and 240 min.

The starch digestion was estimated using eqn (10):

$$\text{Digestion (\%)} = \Delta A \times F \times E_V/\text{W} \times 0.0189 \quad (10)$$

where ΔA is the absorbance reaction read against the reaction blank, F is the conversion from absorbance to μg, *i.e.*, 100 (μg of D-glucose)/GOPOD absorbance, E_V is the extraction volume, W is the weight of the sample analyzed, and 0.0189 is the conversion factor (from free D-glucose, as determined, to anhydro-D-glucose as occurs in starch).

The starch digested at 20 min, 20 to 120 min, and 240 min and remaining undigested after 240 min was considered as RDS, SDS, TDS and RS, respectively. Further, the hydrolysis index (HI) was calculated as the ratio of the area under the hydrolysis curve of the test sample to that of the reference sample (white bread). The expected glycemic index (eGI) was calculated using eqn (11).[29]

$$\text{eGI} = 39.71 + 0.549\ \text{HI} \quad (11)$$

2.6 Statistical analysis

All the experiments were carried out in triplicate, and the data were represented as mean ± standard deviation. The data were evaluated using one-way analysis of variance (ANOVA), and the significant difference among means was determined by the Duncan multiple range test ($p < 0.05$).

3 Results and discussion

3.1 Physical properties of extrudates

The pictographs of the developed rice analogues compared against control rice are given in Fig. 1. The developed rice analogues exhibited a lower length-to-breadth (L/B) ratio (3.26–3.27) compared to the control rice (4.15), classifying them as slender-grain type ($L/B > 3.0$).[30] Despite using larger die openings for producing the rice analogues, the reduced grain size may be attributed to greater shrinkage during drying after extrusion, likely due to higher free water content, which was added during processing and the finer particle size of SRF. These finer particles may compress more easily into compact forms, unlike the natural structure of the control rice. Similar observations for rice analogues were also reported in kodo millet-based formulations.[18]

The bulk density of the developed rice analogues was significantly lower ($p \leq 0.05$) than that of the control commercial rice (Table 1), regardless of the extrusion temperature used. This reduction in bulk density may be attributed to the irregular shape and surface roughness of the analogue rice, which likely led to inefficient packing and increased interstitial air spaces, thereby lowering the overall bulk density. In contrast, the true

Fig. 1 Pictographs of the developed rice analogues and control rice.

Table 1 Physical characteristics of the uncooked rice analogues[a]

Sample	*L–B* ratio uncooked	Bulk density (g mL^{-1})	True density (g mL^{-1})	Porosity (%)	Color values		
					*L**	*a**	*b**
RA 25	3.27 ± 0.17^{b}	0.60 ± 0.05^{a}	3.00 ± 0.31^{a}	80.0 ± 0.08^{a}	71.56 ± 0.50^{a}	5.30 ± 0.10^{a}	16.06 ± 0.25^{b}
RA 50	3.26 ± 0.20^{b}	0.50 ± 0.11^{a}	1.35 ± 0.29^{b}	63.0 ± 0.23^{b}	66.23 ± 1.30^{b}	4.33 ± 0.25^{b}	15.13 ± 0.30^{b}
Control	4.15 ± 0.09^{a}	0.80 ± 0.01^{a}	1.50 ± 0.88^{b}	46.6 ± 0.45^{c}	66.66 ± 0.45^{b}	2.13 ± 0.32^{b}	17.62 ± 0.85^{a}

[a] Values are presented as mean ± standard deviation with different superscripts within a column indicating significant differences; *L–B* ratio: length-to-breadth ratio; *L**: (lightness/darkness); *a**: (redness/greenness); and *b**: (yellowness/blueness); RA 25: extruded rice analogues at 25 °C; RA 50: extruded rice analogues at 50 °C.

density, which reflects the internal structure and material compactness, was higher for RA 25, suggesting greater binding of SRF particles and material shrinkage during drying, resulting in a denser internal matrix. The lower true density observed for RA 50 could be due to the partial swelling of SRF particles under heat, leading to a looser internal arrangement. Additionally, the higher internal compactness observed in the samples might be attributed to increased macronutrient content. The inherently higher true densities of protein and fiber, and their elevated levels in the developed analogues, likely contributed to the higher true density of RA 25. In contrast, partial starch gelatinization in RA 50 during processing might have overridden the influence of macronutrient composition on true density. RA 25 exhibited higher porosity, followed by RA 50 and the control. Extrusion at 25 °C likely trapped more air pockets during extrusion and drying, creating void spaces within the matrix. As a result, though the solid components were dense (high true density), the overall volume might have contained more voids, leading to higher porosity. In contrast, partial starch gelatinization in RA 50 might have increased the mobility of starch and protein to flow and fill the voids, thereby reducing porosity. However, the porosity of the developed analogues was higher than the control rice due to the air voids created during extrusion. Similar results were also reported for the rice analogues from millets and qunioa.[23] The color values of RA 25 and RA 50 were similar, with the exception of the *L** value, which was lower in RA 50 (Table 1). The inherent properties of yellow pea[31] and rice[32] reported in the literature indicated a significantly lower *L** value for rice, with slightly lower and higher *a** and *b** values, respectively. These trends are consistent with the findings of the present study. The slight reduction in *L** observed for RA 50 compared to RA 25 may be attributed to extrusion-induced structural changes, where reduced porosity and a denser matrix could limit internal light scattering, resulting in lower brightness values.[33] The color difference (ΔE) between RA 25 and RA 50 was 5.5, indicating a noticeable visual difference between the two analogue types. A lower ΔE (3.3) between RA 50 and the control rice sample suggests only a slight to moderate color difference. The highest ΔE value (6.0), observed between RA 25 and the control, can be attributed primarily to the inherent color differences between pea starch and natural rice.[34]

3.2 Nutritional content

Moisture content is a critical parameter in rice and rice analogues, as it influences the risk of mold growth and insect infestation. The optimal moisture range for rice grains is between 10% and 14% and the values below 10% may lead to kernel cracking and breakage.[35] Therefore, the moisture content of both extruded samples was standardized at 12% (dry basis) and processed accordingly. The protein content of RA 25 was 11% (db), comparable to that of SRF (12% db)., while the extrusion at 50 °C reduced the protein content to 9.38% db, likely due to slight thermal degradation, potentially reducing nitrogen availability and thus the measurable protein content (Table 2).

Other components, such as fat, ash, and carbohydrates, did not show any major significant differences due to extrusion temperatures, as these compounds are generally more heat-stable. The rice analogues from both extrusion methods exhibited significantly different proximate compositions compared to the control rice sample, particularly in their higher protein content, indicating the nutritional superiority of SRF as a raw material. However, high-temperature extrusion might negatively impact this protein content. Further evaluation of other functional properties under different extrusion conditions would provide a better understanding of the suitability of these methods for rice analogue production.[35] Thus, the SRF could be a potential ingredient to make rice analogues with enhanced nutritional values.

Table 2 Proximate compositions of uncooked rice analogues[a,b]

Sample	Moisture (%)	Protein (%)	Fat (%)	Ash (%)	Carbohydrate (%)
RA 25	12.26 ± 0.07^{b}	10.96 ± 0.02^{a}	1.58 ± 0.20^{a}	2.69 ± 0.23^{a}	74.76 ± 0.11^{b}
RA 50	11.30 ± 0.38^{a}	9.38 ± 0.20^{b}	1.37 ± 0.25^{a}	2.67 ± 0.17^{a}	75.57 ± 0.08^{b}
Control	12.02 ± 0.21^{b}	2.98 ± 0.14^{c}	0.69 ± 0.40^{b}	2.69 ± 0.31^{a}	81.63 ± 0.13^{a}

[a] Values are presented as mean ± standard deviation with different superscripts within a column indicating significant differences. [b] All the values are in a dry basis; RA 25: extruded rice analogues at 25 °C; RA 50: extruded rice analogues at 50 °C; RA 25: extruded rice analogues at 25 °C; RA 50: extruded rice analogues at 50 °C.

3.3 Functional properties

3.3.1 Water absorption (WAI) and solubility index (WSI). The WAI was measured to determine the potential of rice analogues to absorb water in the kernels while maintaining the structure.[27] Concomitantly, the WSI defines the extent of starch degradation during the extrusion, as it is associated with the increase in water-soluble polysaccharides such as amylose.[23] As presented in Table 3, the WAI of the RA 50 was significantly higher than that of RA 25. This may be attributed to the partial swelling of starch granules during high-temperature extrusion, which leads to the disruption of intermolecular bonds and increased water-binding sites. Although the WSI did not differ significantly between RA 25 and RA 50, the slightly higher value observed in RA 50 suggests damage to the crystalline arrangement in starch, facilitating greater leaching of soluble components upon water exposure. Both extruded samples exhibited higher WAI and WSI values compared to the control rice, indicating enhanced water accessibility and reduced interparticle cohesion in the analogues relative to the native rice structure. The potential presence of fiber in SRF could also significantly contribute to the water absorption compared to the polished control rice. Similarly, Wang *et al.* (2021)[10] observed a 3 g g^{-1} and 4% increase in the WAI and WSI of purple sweet potato-based rice analogues, respectively. Karthik *et al.* (2024)[18] also reported that the WSI of the control raw rice was lower than that of the developed rice analogues because of the compact structure of raw rice that resisted the solubilization of components, unlike the rice analogues.

3.3.2 Crystallinity. The X-ray diffractograms presented in Fig. 2 indicate that the control rice sample exhibited distinct 2θ peaks at approximately 15°, 17° and 23°, which are characteristic of an A-type crystalline pattern.[23] In contrast, both developed rice analogues, regardless of the extrusion method, displayed a notable 2θ peak around 5°, along with 2θ peaks at approximately 15°, 17°, 20°, and 22°, confirming the presence of a typical C-type crystalline structure. Notably, the intensity of the peak at 22° was slightly lower in RA 50, corresponding with its significantly reduced relative crystallinity compared to RA 25 and the control. This reduction is likely due to partial disruption of the crystalline regions at high temperatures.[10] Budi *et al.* (2015)[36] and Wang *et al.* (2021)[10] observed the formation of V-type crystals in extruded corn starch and purple sweet potato-based rice analogues, respectively, attributed to amylose leaching and amylose–lipid complex formation at extrusion temperatures exceeding 50 °C. This suggests that the temperature applied during RA 50 processing was insufficient to fully gelatinize the starch or release enough amylose to facilitate significant lipid complexation and alter the crystalline structure. However, the presence of small 2θ peaks around 13° and 19–20° in the analogue samples, which are typically associated with V-type crystallinity, might arise from the inherently higher amylose content in pulses relative to rice, allowing the formation of some amylose–lipid complexes.

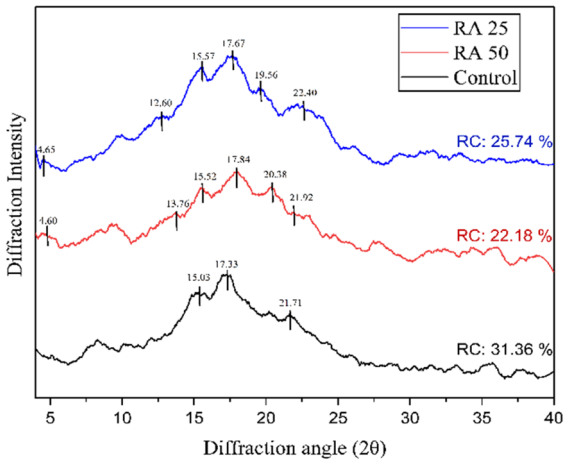

Fig. 2 Crystalline properties of uncooked rice analogues; RC: relative crystallinity.

3.3.3 Fourier transform infrared spectroscopy (FTIR). The FTIR spectra of SRF-based rice analogues and control rice are presented in Fig. 3. The broad absorption band in the range of 3000–3600 cm^{-1} corresponds to the O–H stretching vibrations, which are primarily attributed to hydroxyl groups present in starch and in the side chains of certain amino acids such as serine, threonine, and tyrosine in proteins. The peak observed at 2930 cm^{-1} is associated with the C–H stretching vibrations, originating from both starch and the alkyl side chains of proteins. The band near 1650 cm^{-1} represents the amide I region, primarily arising from C=O stretching vibrations in peptide and iso-peptide bonds, which reflects the protein backbone structure. Notably, the intensity of this peak was higher in the extruded samples compared to the control rice, in agreement with the higher protein content of the SRF used in formulation. Furthermore, the absorption bands at approximately 1048 cm^{-1} and 1022 cm^{-1} correspond to the crystalline and amorphous regions of starch granules, respectively. The comparatively lower intensity of the 1048 cm^{-1} band in RA 50 suggests a reduction in crystalline order, which aligns with the XRD findings. Overall, the spectral profiles of rice analogues were similar to that of control rice, with no additional peaks observed, indicating that no new functional groups or chemical transformations occurred in the developed rice analogues.[23] These observations are in agreement with recent studies[10,16] on FTIR analysis of purple sweet potato- and soybean-based rice analogues.

3.3.4 Thermal characteristics. The thermograms of the developed rice analogues are compared with the control in

Table 3 Effect of extrusion temperature on the water absorption (WAI) and water solubility (WSI) indices of the uncooked rice analogues[a]

Sample	WAI (g g^{-1})	WSI (%)
RA 25	2.27 ± 0.02[b]	0.03 ± 0.01[a]
RA 50	3.65 ± 0.40[a]	0.09 ± 0.03[a]
Control	1.77 ± 0.71[c]	0.01 ± 0.002[a]

[a] Values are presented as mean ± standard deviation with different superscripts within a column indicating significant differences; RA 25: extruded rice analogues at 25 °C; RA 50: extruded rice analogues at 50 °C.

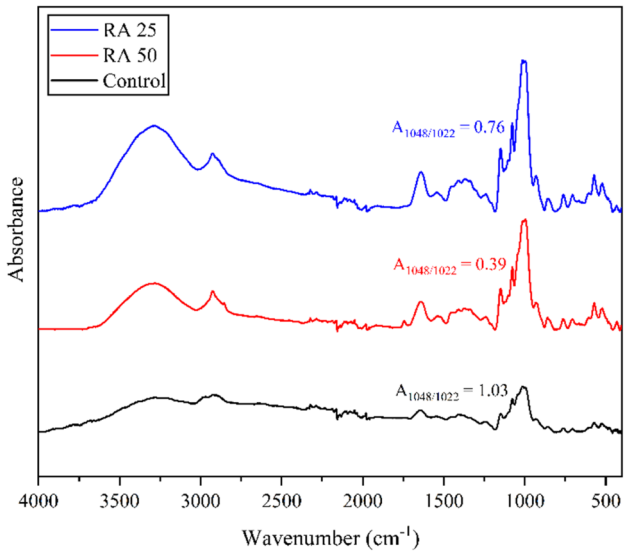

Fig. 3 Fourier transform infrared (FTIR) spectra of uncooked rice analogues.

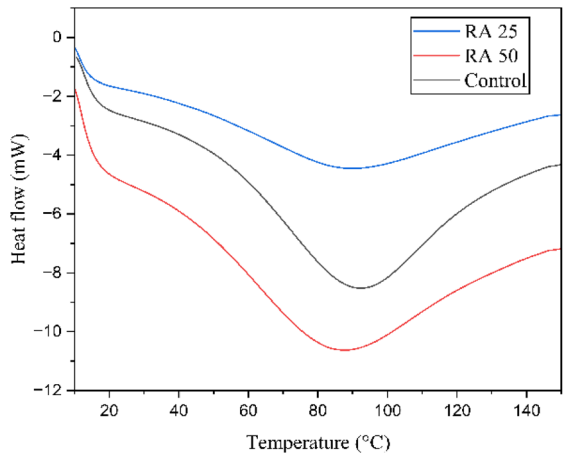

Fig. 4 Differential scanning calorimetry (DSC) curves of uncooked rice analogues.

Fig. 4 and the gelatinization temperatures are given in Table 4. Both rice analogues exhibited lower onset (T_o) and peak (T_p) gelatinization temperatures compared to the control. Additionally, RA 50 showed lower gelatinization temperatures than RA 25. The reduction relative to the control could be due to differences in the crystalline structure between pulse and rice starches. The gelatinization is generally initiated in amorphous regions of amylopectin and gradually affects the double helical crystalline arrangement. Rice starch typically has fewer amorphous regions and a compact amylopectin arrangement, making gelatinization initiation more difficult, which could have resulted in a higher T_o.[37] In contrast, the pea starch has a higher proportion of amorphous regions and a weaker crystalline arrangement, leading to lower T_o.[38] However, the higher amylose content in pea starch could form dense helical structures that increase resistance to gelatinization. This resistance broadens the gelatinization temperature range, increasing the conclusion temperature (T_c) and gelatinization temperature range (ΔT). Previous studies have also correlated higher ΔT values with amylose content.[39,40] The difference between RA 25 and RA 50 could suggest that heat during extrusion has disrupted the amylopectin structure, facilitated easier gelatinization,[41] and thus lowered T_o. Since the extrusion conditions in the current study are unlikely to cause significant depolymerization, the similar behavior of amylose in RA 50 and RA 25 accounts for their comparable T_p and T_c values. The reduced gelatinization enthalpy (ΔH) observed in rice analogues compared to the control and between RA 25 and RA 50 further reflects differences in relative crystallinity. Budi *et al.* (2015) also reported an overall loss in the gelatinization peaks for corn starch and corn flour-based rice analogues produced at higher extrusion temperatures (>70 °C) and elevated moisture contents (35–45%) due to the complete disruption of the starch granules during extrusion. It is to be noted that though the altered chains could reorganize during further drying, the reordered structures are generally not strong enough compared to the native ones. Hence, the reduction in thermal stability is inevitable.

3.4 Cooking characteristics

The cooking parameters, namely, cooking time, water absorption ratio, solid loss due to cooking, and elongation ratio, of the developed rice analogues are provided in Table 5. The cooking time for the rice analogues (2–12 min) was significantly lower than that of the control rice (20 min). Karthik *et al.* (2024)[18] also reported significantly reduced cooking time (6–8 min) for kodo millet-based rice analogue in comparison to commercial rice. RA 50 exhibited a significantly shorter cooking time (2 min) compared to RA 25, which required 12.5 min. Both extruded samples showed reduced cooking times relative to the control rice (20 min), which can be attributed to the use of pre-ground flour in their formulation. This pre-processing step enhances the water absorption rate during cooking due to the absence of

Table 4 Effect of extrusion temperature on the gelatinization properties of uncooked rice analogues[a]

Sample	T_o (°C)	T_p (°C)	T_c (°C)	ΔT (°C)	ΔH (J g^{-1})
RA 25	37.93 ± 0.63^b	89.95 ± 1.02^b	147.26 ± 2.14^a	109.33 ± 1.72^b	18.91 ± 0.63^b
RA 50	33.48 ± 0.91^c	87.06 ± 0.75^c	147.25 ± 2.43^a	113.77 ± 1.38^a	16.63 ± 0.56^c
Control	47.29 ± 1.17^a	92.36 ± 0.56^a	145.42 ± 1.96^b	98.13 ± 1.09^c	21.82 ± 0.78^a

[a] Values are presented as mean ± standard deviation with different superscripts within a column indicating significant differences; T_o: onset temperature; T_p: peak temperature; T_c: conclusion temperature; ΔT: degree of heterogeneity; ΔH: gelatinization enthalpy; RA 25: extruded rice analogues at 25 °C; RA 50: extruded rice analogues at 50 °C.

Table 5 Cooking characteristics of the extruded rice analogues[a]

Sample	Cooking time (min)	Water absorption ratio	Solid loss (%)	Elongation ratio
RA 25	12.5 ± 0.35[b]	1.53 ± 0.01[c]	3.25 ± 0.35[a]	0.93 ± 0.07[b]
RA 50	1.90 ± 0.14[c]	2.89 ± 0.11[b]	3.65 ± 0.21[a]	1.06 ± 0.10[a]
Control	20.5 ± 0.70[a]	3.13 ± 0.03[a]	2.5 ± 0.70[b]	1.21 ± 0.03[a]

[a] Values are presented as mean ± standard deviation with different superscripts within a column indicating significant differences; RA 25: extruded rice analogues at 25 °C; RA 50: extruded rice analogues at 50 °C.

the dense, intact structure present in native rice kernels. In particular, the markedly lower cooking time of RA 50 might be explained by the partial gelatinization of starch that occurs during extrusion at 50 °C. High temperatures could disrupt the crystalline structure of starch granules, making them more amenable to rapid water uptake and swelling during cooking. Consequently, RA 50 reached the desired soft texture more quickly. This is more evident from the higher WAR of RA 50 compared to RA 25. However, the WAR of control rice was higher than those of both extruded samples. In general, the native rice (cereal grains) has higher amylopectin than peas (pulses). Amylopectin is directly related to the swelling capacity of the grain, resulting in a higher WAR ratio of control rice.[42] The solid loss (cooking loss) of all extruded rice analogues was significantly higher than that of the control rice sample, with no statistically significant difference observed due to extrusion temperature. Similar to the trend observed in WSI, RA 50 exhibited a slightly higher value. This could be attributed to greater amylose leaching, likely due to increased water uptake resulting from the disruption of crystalline starch structures during hot extrusion. A higher solid loss of millet-based rice analogues compared to control rice was also reported.[18] Solid loss is one of the vital cooking properties as it determines the degree of structural breakdown in extruded products that occurs during cooking.[23] A higher solid loss in the extruded rice analogues suggests disturbed structural integrity and cooking stability. This further highlights the requirement for modification of pea starch to be a suitable base material for developing extruded rice analogues with minimal nutrient leaching and improved cooking performance. The elongation ratio of the RA 50 sample was significantly higher than that of RA 25. However, both extruded rice analogue samples exhibited lower elongation ratios compared to the control rice. This reduction may be attributed to the greater swelling capacity of native rice starch relative to pea starch. Additionally, as noted in Section 3.1, the uncooked rice analogue kernels were smaller in size, reflected by their lower length-to-breadth (L/B) ratios. The combination of a smaller kernel size and the inherently lower swelling power of pea starch granules likely contributed to the reduced elongation during cooking. The higher elongation ratio of RA 50 than RA 25 could be explained by the enhanced water absorption capacity resulting from the disruption of crystalline regions during hot extrusion. This structural modification may have allowed amylopectin chains to bind more water, facilitating greater elongation. These results were similar to those reported in ref. 23 for low glycaemic index rice analogues made using millet-mix-based ingredients.

3.4.1 Texture of cooked rice analogues. Textural properties play a vital role in determining the sensory quality and consumer acceptability of the developed rice analogues. Different textural parameters, namely, hardness, adhesiveness, springiness, cohesiveness, gumminess, chewiness and resilience for all the samples, are listed in Table 6. The hardness of RA 50 was comparable to that of the control sample, with values ranging from 67 to 79 N. The higher hardness in RA 25 could be attributed to the low water absorption and cooking tendency.[43] The adhesiveness or the stickiness of rice during decompression is another important textural property for rice and rice analogues. It followed the order of control > RA 50 > RA 25. The higher adhesiveness observed in the control rice may be attributed to its greater gelatinization potential. In RA 50, partial starch gelatinization during extrusion likely enhanced its ability to gelatinize during cooking, resulting in a moderately sticky texture compared to RA 25.

The springiness of the control sample showed higher values (0.74), followed by RA 50 (0.71) and RA 25 (0.69). This indicates that the elasticity of the developed rice analogues was slightly reduced but could still allow comparable mastication to control while eating.[44] The cohesiveness, which indicates a sample's ability to withstand repeated compression, was highest in RA 25, followed by RA 50 and the control. A similar trend was observed for gumminess and chewiness, which are indicators of

Table 6 Textural properties of the cooked rice analogues[a]

Sample	Hardness (N)	Adhesiveness (N.s)	Springiness (mm)	Cohesiveness	Gumminess	Chewiness (g)	Resilience
RA 25	199.32 ± 0.86[a]	−0.04 ± 0.03[c]	0.69 ± 0.06[a]	0.73 ± 0.12[a]	145.65 ± 0.41[a]	97.41 ± 0.68[a]	0.47 ± 0.12[a]
RA 50	67.28 ± 0.66[c]	−0.30 ± 0.01[b]	0.71 ± 0.10[a]	0.66 ± 0.02[a]	45.19 ± 0.85[b]	32.96 ± 0.57[b]	0.42 ± 0.04[a]
Control	79.83 ± 0.78[b]	−7.44 ± 0.28[a]	0.74 ± 0.13[a]	0.53 ± 0.04[a]	42.37 ± 0.23[c]	31.69 ± 0.69[b]	0.36 ± 0.03[a]

[a] Values are presented as mean ± standard deviation with different superscripts within a column indicating significant differences; RA 25: extruded rice analogues at 25 °C; RA 50: extruded rice analogues at 50 °C.

the effort required to disintegrate the food. This may be linked to the higher hardness exhibited by RA 25. Resilience, reflecting the ability of a sample to recover its shape after deformation, showed a trend consistent with springiness, with no significant differences among the tested samples.[45] Therefore, SRF-based hot extrusion produces rice analogues with more desirable textural properties than commercial rice and holds the potential to be employed at a commercial scale.

3.4.2 Morphology. Fig. 5 presents the SEM images of the cross-sectioned, uncooked rice analogues and control rice. In RA 25, the starch granules appeared closely bound with some gaps, contributing to the formation of a compact rice-shaped structure. This packed granular structure may explain the lower water absorption and longer cooking time observed. In contrast, RA 50 exhibited swollen starch granules with visible internal cracks, likely resulting from the rapid vaporization of moisture during extrusion. As the heated SRF dough at 50 °C temperature exited the die, the sudden release of steam could have caused expansion and bubble formation. The growth and collapse of these bubbles could lead to the development of cracks within the extrudate. These structural cracks along with preswollen starch granules enhanced water absorption, facilitating faster cooking. Moreover, the internal morphology of RA 50 was comparable to that of control rice. Similar observations for rice analogues made using modified cassava flour and rice flour were reported, suggesting that the cracks in between the structures could create channels for water penetration while cooking.[11] These cracks were related to the reduced cooking time of rice analogues made from the broken rice, foxtail millet, barnyard millet, and quinoa.

The effect of cooking on the morphology of the extruded samples and control rice is illustrated in Fig. 4g–l. RA exhibited swollen starch granules, whereas RA 50 displayed a fully gelatinized structure closely resembling that of control rice.[23] This morphological similarity is consistent with the comparable water absorption ratio observed between RA 50 and the control sample. Studies involving rice analogues developed from sago-mung bean-corn flour mixtures and canihua (*Chenopodium pallidicaule Aellen*), respectively, have also highlighted the effectiveness of hot extrusion in producing rice analogues with characteristics similar to those of natural rice.[46,47] These findings support the conclusion that hot extrusion yields rice analogues with more favorable morphological properties. Therefore, the chemical composition of ingredients and extrusion type play a crucial role in determining the thermal properties of the rice analogues.[8] Moreover, the lowered gelatinization temperatures and enthalpies observed in the current study could unlock the quick-cooking potential of the developed rice analogues, aligning with the findings in Section 3.4.

3.5 *In vitro* digestibility

The *in vitro* starch digestibility parameters, namely, rapidly digestible starch (RDS), slowly digestible starch (SDS), total

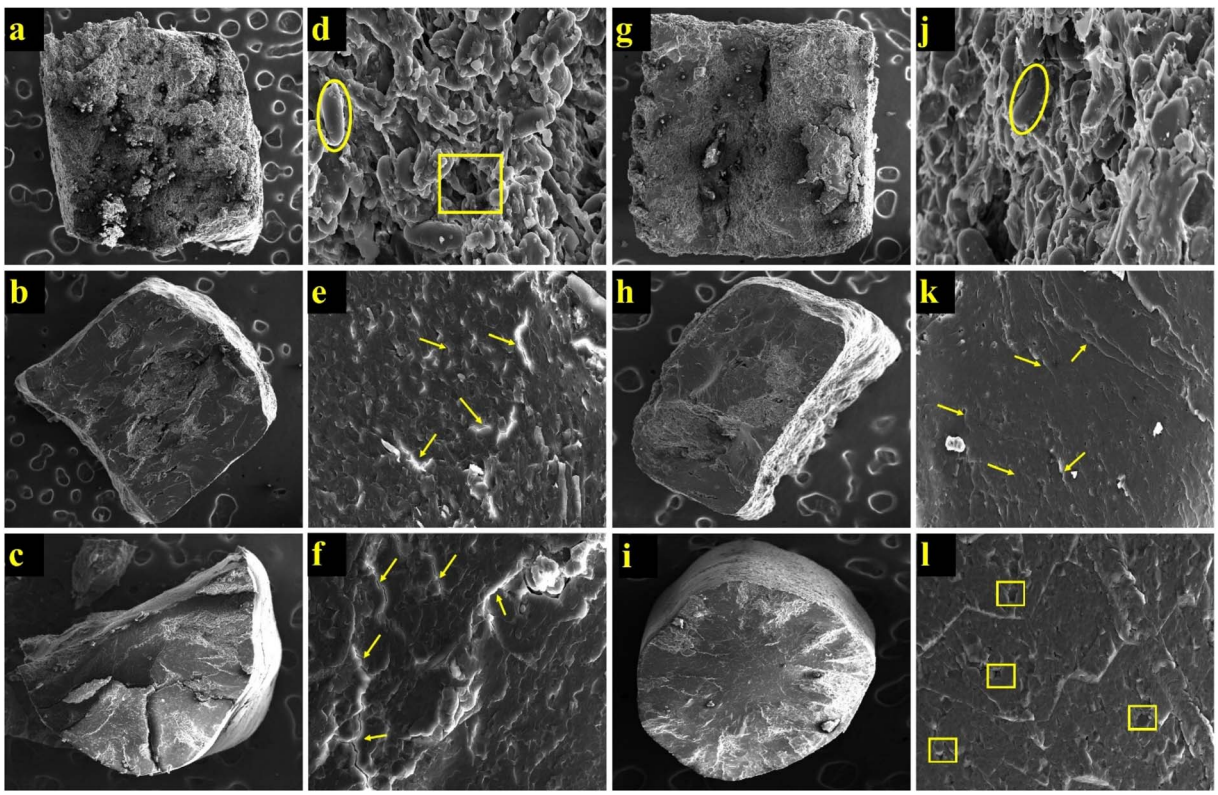

Fig. 5 Scanning electron microscopy (SEM) images for uncooked and cooked rice analogues. (a): uncooked RA 25 at 100×; (b): uncooked RA 50 at 100×; (c): uncooked control at 100×; (d): uncooked RA 25 at 2000×; (e): uncooked RA 50 at 2000×; (f): uncooked control at 2000×; (g): cooked RA 25 at 100×; (h): cooked RA 50 at 100×; (i): cooked control at 100×; (j): cooked RA 25 at 2000×; (k): cooked RA 50 at 2000×; (l): cooked control at 2000×. ⬯ – starch granule; ◥ – cracks; ▭ – voids or gaps.

Table 7 *In vitro* starch digestibility of the rice analogues[a]

Sample	RDS (%)	SDS (%)	TDS (%)	RS (%)	HI (%)	eGI
RA 25	32.99 ± 0.06[a]	28.78 ± 0.05[c]	63.75 ± 0.12[c]	15.01 ± 0.26[a]	72.48 ± 0.49[c]	75.83 ± 1.03[c]
RA 50	32.21 ± 0.01[a]	31.37 ± 0.01[b]	65.58 ± 0.01[b]	11.09 ± 0.03[b]	77.10 ± 0.84[b]	79.07 ± 0.42[b]
Control	28.25 ± 0.01[b]	39.32 ± 0.02[a]	74.69 ± 0.19[a]	7.64 ± 0.02[c]	83.51 ± 0.42[a]	84.53 ± 0.98[a]

[a] Values are presented as mean ± standard deviation with different superscripts within a column indicating significant differences; RDS: rapidly digestible starch; SDS: slowly digestible starch; TDS: total digestible starch; RS: resistant starch; HI: hydrolysis index; eGI: expected glycemic index; RA 25: extruded rice analogues at 25 °C; RA 50: extruded rice analogues at 50 °C.

digestible starch (TDS), resistant starch (RS), and total starch (TS) are presented in Table 7. Typically, pea starch with a C-type crystalline arrangement and higher content of densely coiled amylose is digested more slowly than rice starch, which exhibits an A-type orthorhombic crystalline arrangement.[38] However, in this study, digestibility was assessed after cooking, which could disrupt the crystalline structures and alter digestion behaviour.

The RDS values of rice analogues were greater than those of the control. This higher RDS in rice analogues may be attributed to the amylose chain unwinding that occurs during cooking, thereby increasing enzyme accessibility and the hydrolysis rate. In contrast, the lower amylose levels and more crystalline arrangement in the control resulted in a relatively lower RDS. SDS and TDS followed an order of control > RA 50 > RA 25. The higher values of control might be attributed to the greater starch content compared to rice analogues. The increased values in RA 50 suggest that partial gelatinization during extrusion at 50 °C degraded some resistant starch structures into more slowly digestible forms, thereby increasing SDS and TDS. RS content was higher in rice analogues than in the control. However, this also included undigested protein (cannot produce glucose) and fibre/bran, which in this context was considered RS. The eGI was highest in control, followed by RA 50 and RA 25. The higher starch content and accessible monocyclic structure in rice might have contributed to higher glucose release compared to rice analogues with comparatively lower starch and higher fiber and protein contents. The increased value in RA 50 compared to RA 25 may be due to enhanced digestion in RA 50, contributing to additional glucose release resulting from degradation of resistant starch structures.

4 Conclusions

This study demonstrated the potential of valorising the starch-rich fraction, an underutilized byproduct of pea protein fractionation, into rice analogues through cold extrusion. The developed analogues exhibited enhanced nutritional quality, particularly higher protein and fiber contents, along with reduced gelatinization temperatures and crystallinity compared to conventional rice. These properties resulted in shorter cooking times and desirable textural attributes supporting ready to cook applications, although accompanied by higher solid loss during cooking. Furthermore, the analogues contained greater amounts of slowly digestible and resistant starch, contributing to a lower expected glycemic index. Moreover, the processing temperature played a critical role in determining the final product characteristics. Extrusion at 50 °C further reduced cooking time but compromised nutritional value, crystallinity, and cooking stability relative to 25 °C. Despite these limitations, the overall nutritional profile and glycemic response of the analogues remained superior to conventional rice.

Overall, this study highlights the feasibility of upcycling starch-rich pea byproducts into rice analogues with enhanced nutritional and functional qualities, contributing to sustainability and a circular bioeconomy. It can be concluded that RA25 could serve as a potential substitute for commercial rice providing better nutritional and textural properties. Future research should investigate composite formulations, such as combining rice flour with the starch-rich pea fraction to achieve a balanced essential amino acid profile and further optimize extrusion conditions to minimize cooking losses and assess consumer acceptance of the developed analogues.

Author contributions

Smriti Chaturvedi: conceptualization, methodology, data curation, investigation, resources, writing – original draft, and writing – review & editing; Prudhvi Pasumarthi: methodology, investigation, validation, resources, writing – original draft, and writing – review & editing; Annamalai Manickavasagan: conceptualization, data curation, supervision, resources, validation, and writing – review & editing; Mathad P. F.: methodology and resources.

Conflicts of interest

All the authors who contributed to this work have been acknowledged, and the authors declare no known conflicts of interest for this article.

Data availability

The data will be made available on request.

Acknowledgements

This research was supported by the Natural Sciences and Engineering Research Council of Canada (NSERC). The authors sincerely acknowledge the Canadian Network for Research and Innovation in Machining Technology for facilitating open access publication.

Notes and references

1 R. Kornet, J. Yang, P. Venema, E. van der Linden and L. M. C. Sagis, *Food Hydrocoll.*, 2022, **126**, 107456.
2 M. J. Khan, S. Chaudhary, A. Ali and A. Manickavasagan, *Food Biosci.*, 2025, **68**, 106531.
3 Agriculture and Agri-Food Canada, Canada: Outlook for Principal Field Crops, https://agriculture.canada.ca/en/sector/crops/reports-statistics/canada-outlook-principal-field-crops-2025-07-21#a4, accessed 24 August 2025.
4 T. G. Burger and Y. Zhang, *Trends Food Sci. Technol.*, 2019, 25–33, DOI: 10.1016/j.tifs.2019.02.007.
5 F. Boukid, C. M. Rosell and M. Castellari, *Trends Food Sci. Technol.*, 2021, 729–742, DOI: 10.1016/j.tifs.2021.02.040.
6 J. Thomas, S. G. Gargari and S. Tabtabaei, *Powder Technol.*, 2023, **415**, 118169.
7 P. Pasumarthi, S. Sindhu and M. Annamalai, *Cereal Chem.*, 2024, 1–24.
8 S. Chaturvedi and A. Manickavasagan, *Trends Food Sci. Technol.*, 2024, **148**, 104493.
9 P. K. Haditama, K. Permatasari, N. A. Sukma and M. A. Rian, *Jurnal Pangan dan Agroindustri*, 2022, **10**(3), 178–186.
10 J. Wang, M. Li, C. Wang, Y. Dai, Y. Sun, X. Li, C. G. Heider, X. Wu and J. Liang, *Food Funct.*, 2021, **12**, 739–746.
11 C. Y. Liu, R. Amani, S. Sulaiman, K. Mahmood, F. Ariffin and A. Mohammadi Nafchi, *Food Nutr. Sci.*, 2022, **10**, 1626–1637.
12 L. A. Susi and C. Wibowo, *IOP Conf. Ser. Earth Environ. Sci.*, 2019, **255**, 012012.
13 Z. A. S. Bahlawan, A. C. Kumoro, Megawati and S. K. Wahono, *Curr. Res. Nutr. Food Sci.*, 2023, **11**, 1022–1038.
14 M. Nugraheni, S. Purwanti and P. Ekawatiningsih, *Food Res.*, 2017, **4**(6), 269, DOI: 10.26656/fr.
15 S. Sumardiono, B. Jos, M. F. Z. Antoni, Y. Nadila and N. A. Handayani, *Heliyon*, 2022, **8**, e08969.
16 A. Sutrisno, A. N. F. Suloi, E. S. Murtini and N. A. Bahmid, *Future Foods*, 2024, **10**, 100407.
17 M. Qi, G. Zhang, Z. Ren, Z. He, H. Peng, D. Zhang and C. Ma, *Plant Foods Hum. Nutr.*, 2021, **76**, 26–30.
18 K. V. D. Karthik, B. D. Rao, A. Das, E. Kiranmai, M. Dharini, S. R. Mogulla and D. Sharma, *Future Foods*, 2024, **10**, 100389.
19 N. Singh, N. Kaur, J. C. Rana and S. K. Sharma, *Food Chem.*, 2010, **122**(3), 518–525.
20 A. K. Jukanti, P. A. Pautong, Q. Liu and N. Sreenivasulu, *Trends Food Sci. Technol.*, 2020, **106**, 132–149.
21 A. Mishra, H. N. Mishra and P. Srinivasa Rao, *Food Sci. Technol.*, 2012, 1789–1797, DOI: 10.1111/j.1365-2621.2012.03035.x.
22 A. Ganachari, U. Nidoni, S. Hiregoudar, K. T. Ramappa, N. Naik, S. Vanishree and P. F. Mathad, *J. Food Sci. Technol.*, 2022, **59**(8), 3150–3157.
23 G. P. Yadav, C. G. Dalbhagat and H. N. Mishra, *J. Food Process. Preserv.*, 2021, **45**, 1–11.
24 N. Singh, L. Kaur, N. Singh Sodhi and K. Singh Sekhon, *Food Chem.*, 2005, **89**, 253–259.
25 AOAC, *Official Methods of Analysis*, 18th edn, 2007.
26 M. Cermeño, J. V. C. Silva, M. Arcari and C. Denkel, *LWT–Food Sci. Technol.*, 2024, **198**, 115948.
27 S. N. Tabas, M. S. Noghabi, A. M. Dovom and M. Davtalab, *Food Nutr. Sci.*, 2023, 5873–5881.
28 H. N. Englyst and G. J. Hudson, *Food Chem.*, 1996, **57**, 15–21.
29 I. Goñi, A. Garcia-Alonso and F. Saura-Calixto, *Nutr. Res.*, 1997, **17**(3), 427–437.
30 S. Nath, P. Bhattacharjee, S. Bhattacharjee, J. Datta and A. K. Dolai, *Appl. Food Res.*, 2022, **2**, 100067.
31 S. Vatansever and C. Hall, *J. Supercrit. Fluids*, 2020, **156**, 104659.
32 G. P. Yadav, C. G. Dalbhagat and H. N. Mishra, *Int. J. Food Sci. Nutr. Eng.*, 2022, **4**(1), 30–43.
33 A. V. Malinka, *J. Quant. Spectrosc. Radiat. Transf.*, 2014, **141**, 14–23.
34 B. Saberi, Q. V. Vuong, S. Chockchaisawasdee, J. B. Golding, C. J. Scarlett and C. E. Stathopoulos, *J. Food Process. Preserv.*, 2016, **40**, 1339–1351.
35 K. A. Millar, E. Gallagher, R. Burke, S. McCarthy and C. Barry-Ryan, *J. Food Compos. Anal.*, 2019, **82**, 103233.
36 F. S. Budi, P. Hariyadi, S. Budijanto and D. Syah, *J. Dev. Sustain. Agric.*, 2015, **10**, 91–100.
37 S. Srichuwong and J. I. Jane, *Food Sci. Biotechnol.*, 2007, **16**(5), 663–674.
38 Q. Ouyang, X. Wang, Y. Xiao, F. Luo, Q. Lin and Y. Ding, *Food Chem.*, 2021, **358**, 129858.
39 P. Pasumarthi, N. Malleshi and A. Manickavasagan, *Food Chem.*, 2025, **466**, 142216.
40 P. Pasumarthi and A. Manickavasagan, *Int. J. Biol. Macromol.*, 2025, **331**(2), 148419.
41 P. Pasumarthi and A. Manickavasagan, *Int. J. Biol. Macromol.*, 2025, **318**(3), 144860.
42 C. G. Dalbhagat, D. K. Mahato and H. N. Mishra, *Trends Food Sci. Technol.*, 2019, 226–240, DOI: 10.1016/j.tifs.2019.01.001.
43 K. Zhang, X. Jia, Z. Zhu and W. Xue, *Int. J. Food Prop.*, 2020, **23**(1), 2033–2049.
44 K. Zhang, Y. Tian, C. Liu and W. Xue, *Int. J. Polym. Sci.*, 2020, **2020**(1), 7490505.
45 W. Ramadhan, S. Purwaningsih and S. Nafisah, *Int. J. Food Sci. Technol.*, 2024, **59**, 1770–1780.
46 S. Sumardiono, B. Budiyono, H. Kusumayanti, N. Silvia, V. F. Luthfiani and H. Cahyono, *Foods*, 2021, **10**(12), 3023.
47 A. J. Quispe, M. C. Moreno, A. M. Leon, P. Bouchon and W. T. Medina, *Food Human.*, 2024, **2**, 100193.